



On the influence of the rheological boundary conditions on the fibre orientations in the production of steel fibre reinforced concrete elements

Heiko Herrmann^{a,b*} and Aarne Lees^{a,c}

^a Centre for Nonlinear Studies, Institute of Cybernetics at Tallinn University of Technology, Akadeemia tee 21, 12618 Tallinn, Estonia

^b Institut für Physik, Technische Universität Chemnitz, 09107 Chemnitz, Germany

^c Present address: Department of Mechanical Engineering, University of Rochester, 406 Hopeman Building, Rochester, NY 14627, USA

Received 19 October 2015, accepted 4 December 2015, available online 24 November 2016

© 2016 Authors. This is an Open Access article distributed under the terms and conditions of the Creative Commons Attribution-NonCommercial 4.0 International License (<http://creativecommons.org/licenses/by-nc/4.0/>).

Abstract. In this paper the influence of the boundary conditions on the fibre orientation distribution in rheology simulations of the casting of steel fibre reinforced concrete is discussed. The slip-length of the boundary condition can have a significant influence on the orientation of the fibres. This means that the material and surface properties of the formwork need to be taken into account when designing the casting technology for elements made of steel fibre reinforced concrete. This also implies that there is a chance to influence the fibre orientations by choosing appropriate surface properties of the formwork.

Key words: mechanics, steel fibre reinforced concrete, fibre orientation, rheology simulation, boundary properties.

1. INTRODUCTION

Composite materials are more and more replacing traditional materials in many application areas. Composites include layered materials and fibrous and fibre reinforced materials. Many of these composites have been researched for many years, but also new materials are constantly developed. Short fibre composites are materials in which fibres are mixed into the often brittle matrix material during the production. This mixture is then filled into moulds (e.g. injection moulding of short fibre plastics) or sprayed onto surfaces to strengthen them. Many short fibre composites have been researched for a long time, including their rheological properties [1–9] and are used in everyday products. Although steel fibre reinforced concrete is not a new material at all, the understanding of its properties is not too well developed. For a long time it has mainly been used in industrial floors to prevent cracking.

Composites in general and steel fibre reinforced cementitious composites (SFRCC) are gaining rapidly importance in building industry. Much research has been done on the properties of these materials during

the past decades [10–24]. In short fibre composites, like steel fibre reinforced concrete, the material properties depend on the spatial and orientational distribution of the short fibres. Especially they can become anisotropic and position dependent [12,13,25,26]. The rheology during the production process of the structural parts has influence on the fibre distribution. This has been studied experimentally [27–32] and to a smaller extent also in simulations [25,32,33]. However, the experiments are always based on a specific setup, which is not altered during the experiments, and the simulations seem to be made to reproduce a special experiment. Specifically, this means that the boundary conditions are not changed and different boundary conditions are not compared. It seems to be assumed that the presence of the boundaries alone, not their properties, influence the fibre orientations.

In practice, however, different formwork materials are used, including raw wood and plastic planes as covers and metal plates, also the use of lubricants is possible. As will be shown in the next section, these properties can influence not only the speed with which the cement mass spreads, but also the fibre orientation distribution.

* Corresponding author, hh@cens.ioc.ee

As a result, the surface properties of the formwork and their interaction with the cement mass need to be taken into account in developing casting technologies for SFRCC.

2. RHEOLOGY SIMULATIONS

2.1. Fibre orientation description

The flow of the concrete was simulated as laminar flow. The Herschel–Bulkley viscosity model was used to model a near Bingham fluid-like behaviour for the concrete phase.

The orientation state of fibres at a point in space can be described by a probability distribution function. This function can be expanded in a series of tensors of increasing order [34–37]. To reduce the computational cost, the series can be truncated and a finite set of orientation tensors rather than the probability distribution function can be used to describe the orientation state. In this paper, the second- and fourth-order tensors, a_{ij} and a_{ijkl} , are used to describe the orientation state.

The equation of change for the second-order orientation tensor from [35,38] is used to calculate the evolution of the orientation state:

$$\begin{aligned} \frac{Da_{ij}}{Dt} = & -\frac{1}{2}(\omega_{ik}a_{kj} - a_{ik}\omega_{kj}) \\ & + \frac{1}{2}\lambda(\dot{\gamma}_{ik}a_{kj} + a_{ik}\dot{\gamma}_{kj} - 2\dot{\gamma}_{kl}a_{ijkl}) \\ & + 2D_r(\delta_{ij} - 3a_{ij}), \end{aligned} \quad (1)$$

where $\frac{D}{Dt}$ is the material derivative (co-moving derivative), ω_{ij} is the vorticity tensor, λ is a parameter related to the shape of the particle and is given by $\lambda = (r^2 - 1)/(r^2 + 1)$, and $D_r = C_I \dot{\gamma}$ as suggested in [39]. Here $\dot{\gamma}$ is the scalar magnitude of the rate of the strain tensor, given by

$$\dot{\gamma} = |\dot{\gamma}_j| = \sqrt{\frac{1}{2}(\dot{\gamma}_j \dot{\gamma}_{ji})}, \quad (2)$$

where C_I is the fibre–fibre interaction coefficient which serves to randomize the orientation state. The correlation used to calculate C_I depends on the fibre volume fraction Φ and aspect ratio r :

$$C_I = C_I(\Phi, r), \quad (3)$$

$$\Phi = nL \frac{\pi D^2}{4}, \quad (4)$$

$$r = \frac{L}{D}, \quad (5)$$

where L is the fibre length, D is the diameter, and n is the fibre number density. According to [38], two cases were distinguished:

$$C_I = \begin{cases} 0.03(1 - e^{-0.224\Phi r}) & \text{if } \Phi r \leq 1.3 \\ 0.0184e^{-0.7148\Phi r} & \text{if } \Phi r > 1.3 \end{cases}. \quad (6)$$

Since the equation of change for the second-order orientation tensor contains the fourth-order orientation tensor, a closure approximation that allows the calculation of a_{ijkl} from a_{ij} is required. The IBOF-5 closure approximation suggested in [40] is used here. The IBOF-5 approximation is given by

$$\begin{aligned} a_{ijkl} = & \beta_1 S(\delta_{ij}\delta_{kl}) + \beta_2 S(\delta_{ij}a_{kl}) + \beta_3 S(a_{ij}a_{kl}) \\ & + \beta_4 S(\delta_{ij}a_{km}a_{ml}) + \beta_5 S(a_{ij}a_{km}a_{ml}) \\ & + \beta_6 S(a_{im}a_{mj}a_{kn}a_{nl}), \end{aligned} \quad (7)$$

where $S(T_{ijkl}) = \frac{1}{24} \sum_{\text{perm}(ijkl)} T_{ijkl}$ is the symmetrization operator, with the sum carried out over all permutations of $ijkl$, and the coefficients β are functions of the second and third invariants of a_{ij} (see [40]).

2.2. Numerical solver implementation

For the simulation the interFoam solver from the OpenFOAM 2.3.0 library was used. The solver uses the so-called Weller volume of fluid method [41] to simulate multiphase free-surface flow. The solver was extended to include calculations of the equation of change for the second-order fibre orientation tensor field in the concrete phase. At every time-step, Eq. (1) was solved to simulate the evolution of the fibre orientation tensors in the concrete phase. The simulation is one-way coupled – the flow-field affects the fibre orientation distribution, whereas the fibre orientation has no effect on the flow field.

Since the fibres are present only in the concrete phase, a boundary condition for the orientation tensors is required at the concrete–air interface. In the cells where the phase fraction of the concrete phase dropped below a certain value, the fibre orientation tensors were forced to a value representing a completely isotropic orientation state. This effectively imposed a fixed value boundary condition on the fibre orientation at the concrete–air interface.

2.3. Simulation and boundary conditions

The first case simulated was a rectangular concrete slab being poured from a circular pipe at one corner of the slab. The geometry of the slab is $W \times L \times H$: 1.2 m \times 1.2 m \times 0.15 m, the inlet has a diameter of \varnothing 14 cm and is located in one corner 25 cm from the side walls (Fig. 1). This is the same geometry as presented at the 4C-Flow homepage [42], which also shows some results that could be used for an initial verification.

At the inlet, a velocity profile was imposed on concrete entering the domain with fibres aligned with the pipe axis and a zero gradient boundary condition for the pressure.

To the atmosphere above the mould, fixed total pressure and a zero gradient boundary condition for the velocity were applied.

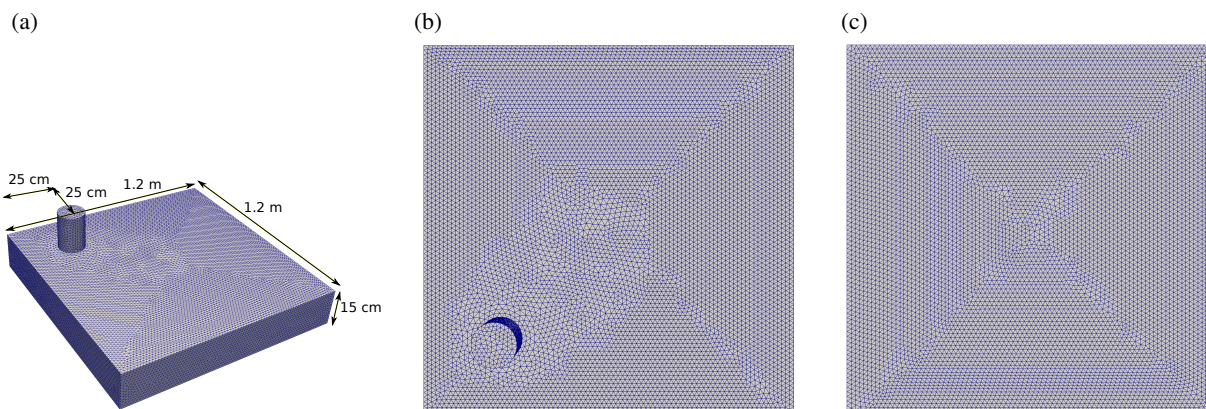


Fig. 1. The geometry and mesh of the verification simulation. The mesh has 384 509 cells. (a) Geometry: $W \times L \times H$: 1.2 m \times 1.2 m \times 0.15 m, inlet \varnothing 14 cm, located 25 cm from the side walls; (b) top view of the mesh; (c) bottom view of the mesh.

At the walls of the mould, a zero gradient condition was applied to the pressure field, while a planar state of orientation in the plane of the walls was assumed for the fibres. The influence of slip at the walls on the final orientation state was investigated using a Navier slip boundary condition with varying slip lengths similarly to the studies conducted in [33]. The different slip lengths used in the Navier slip boundary conditions were 0, 8 cm, and infinite slip length.

An initial verification of the simulations was performed by visual comparison of the result with the available simulation results of 4C-Flow [42], which are in good agreement for the slip length of 8 cm. Also, the simulation is in reasonable agreement with the fibre orientations obtained from measurements of fibre orientations in full-size floor slabs [19,20,43].

Further simulations were performed with long single-span slabs, cast from different points. The geometry in these cases was $W \times L \times H$: 1 m \times 5 m \times 0.25 m.

3. RESULTS AND DISCUSSION

Figure 2 shows the local fibre orientation distributions represented by orientation glyphs, in this case ellipsoids. A sphere represents isotropic distribution, a very elongated glyph represents an area where fibres are very well aligned with each other, and a lens- or penny-shaped glyph represents a distribution in which the fibres are mostly oriented within a plane.

As can be seen in Fig. 2, different boundary conditions produce different orientation distributions of the fibres. In Fig. 2a,d, which were simulated with a no-slip boundary, the fibres are well aligned in the flow direction especially in the bottom layer, while in Fig. 2b,e, which were calculated with a slip length of 0.08 m, the fibres

are relatively well aligned perpendicular to the flow direction. This is even more apparent in Fig. 2f, which was calculated with an infinite slip length. Figure 3 shows a close-up of the bottom layer in the same orientation as Fig. 2d–f; this figure also shows the flow vectors. The difference can be explained by the fact that with a no-slip boundary, new fibres are transported to the front with the concrete mass in the top layer of the flow, while with a slip or slip-length boundary condition, the same concrete mass and fibres are at the front for a longer time and there is a stretching of the mass perpendicular to the flow direction for some time.

4. CONCLUSION

The simulations show that the influence of the boundary properties on the fibre orientations can be strong. This means that an unintentional change in the boundary, e.g. a rough wooden plank in between smooth planks, could cause an unintentional and unexpected change in the fibre orientations compared to predictions. This change could weaken the whole structural element. On the other hand, intentional variations in the boundary properties could be used to willingly influence the fibre orientations. This means that the formwork properties should be taken into account when designing casting technologies, not only in terms of the speed of spreading but also with respect to the fibre orientations, and it could mean that in certain conditions a rough surface, which slows the spreading down, is actually to be preferred over a slippery one, because of the fibre orientation distribution.

Thus, to summarize, the influence of the surface properties of the formwork on the fibre orientation distribution should be studied, as it presents both a danger and a chance at the same time for developing casting technologies of SFRCC.

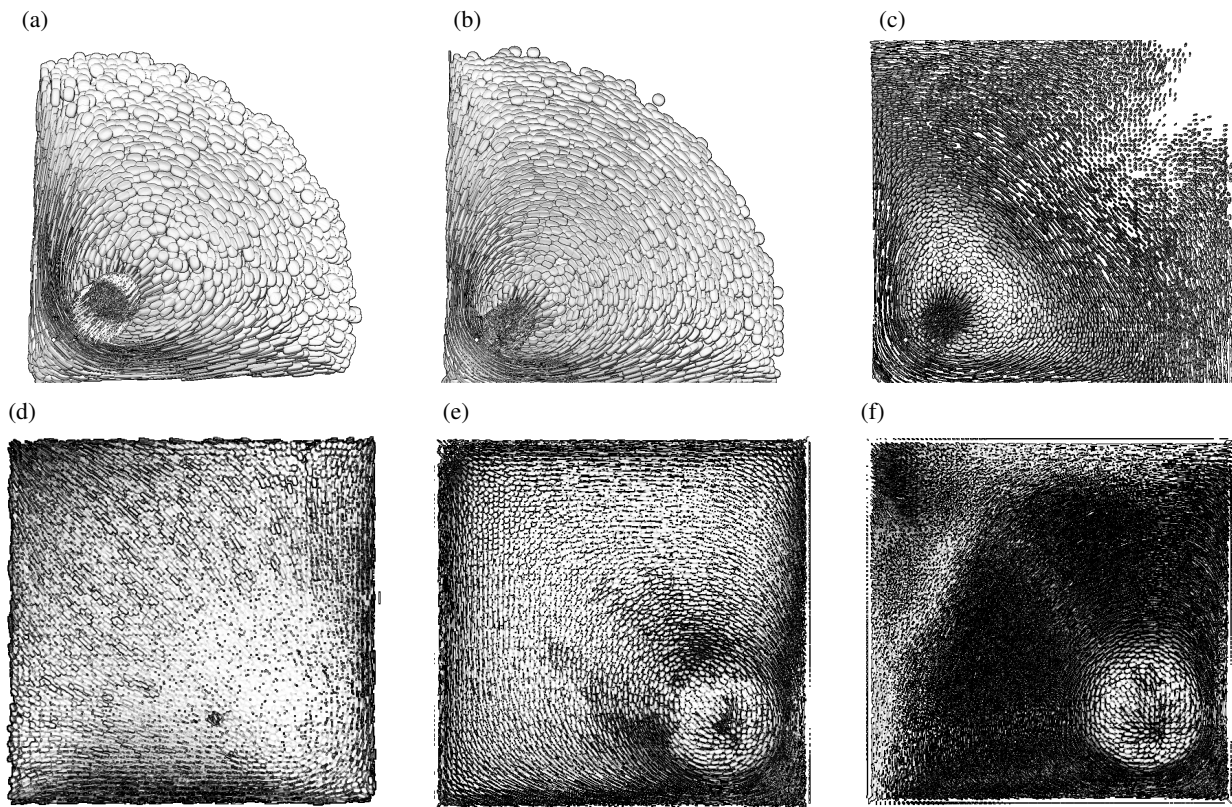


Fig. 2. Results of the rheology simulation. The glyphs represent the alignment of the fibres with each other, where a sphere represents isotropy and cigar-shaped fibres that are well aligned with each other. (a) No slip at $t = 5$ s, top view; (b) slip length 0.08 m at $t = 5$ s, top view; (c) slip at $t = 5$ s, top view; (d) no slip at $t = 14$ s, bottom view; (e) slip length 0.08 m at $t = 14$ s, bottom view; (f) slip at $t = 14$ s, bottom view.

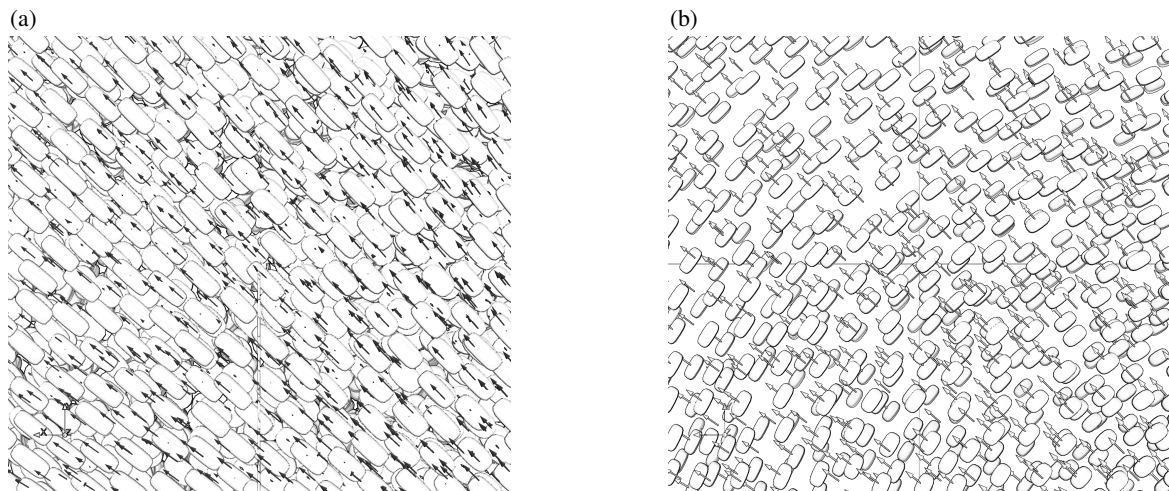


Fig. 3. Close-up of the bottom layer with flow vectors. Inflow is from the lower right, outside the image. It is noteworthy that with the slippery formwork the fibres align mostly perpendicular to the flow direction in the bottom layer. (a) No slip; (b) slip length 0.08 m.

ACKNOWLEDGEMENTS

This research was supported by the European Union through the European Regional Development Fund, in particular through funding for the “Centre for Nonlinear Studies” as an Estonian national centre of excellence. It was compiled with the assistance of the Tiger University Program of the Estonian Information Technology Foundation (VisPar/Kyb3 visualization system, EITSA/HITSA grants 10-03-00-24, 12-03-00-11, and 13030009). Support by the German Academic Exchange Service in the form of three DAAD-RISE Fellowships for visiting interns and by the Estonian Research Council (PUT1146) is gratefully acknowledged.

The simulations were made on the TUT HPC cluster, which was financed by the Archimedes Foundation through the ETAIS project, a joint project between the University of Tartu, Tallinn University of Technology, NICPB, and EENet.

The authors are grateful to J. Schnell and the anonymous referee for their fast and positive response.

The publication costs of this article were covered by the Estonian Academy of Sciences.

REFERENCES

1. Chung, S. T and Kwon, T. H. Numerical simulation of fiber orientation in injection molding of short-fiber-reinforced thermoplastics. *Polym. Eng. Sci.*, 1995, **35**(7), 604–618.
2. McLeod, M. A. *Injection Molding of Pregenerated Microcomposites*. Virginia Polytechnic Institute and State University, 1997. Available from <http://scholar.lib.vt.edu/theses/available/etd-0898-145634/> (accessed 17 October 2015).
3. Nabialek, J. Modeling of fiber orientation during injection molding process of polymer composites. *Kompozyty*, 2011, **11**(4), 347–351.
4. Park, J. M. and Park, S. J. Modeling and simulation of fiber orientation in injection molding of polymer composites. *Math. Probl. Eng.*, 2011, **2011**, ID 105637.
5. Vélez-García, G. M. *Experimental Evaluation and Simulations of Fiber Orientation in Injection Molding of Polymers Containing Short Glass Fibers*. Virginia Polytechnic Institute and State University, 2012. Available from http://scholar.lib.vt.edu/theses/available/etd-04262012-100846/unrestricted/Velez.Garcia_GM_2012.pdf (accessed 17 October 2015).
6. VerWeyst, B. E., Tucker, III C. L., Foss, P. H., and O’Gara, J. F. Fiber orientation in 3-D injection molded features: prediction and experiment. *Int. Polym. Proc.*, 1999, **14**(4), 409–420.
7. Andrić, J., Lindström, S. B., Sasic, S., and Nilsson, H. Rheological properties of dilute suspensions of rigid and flexible fibers. *J. Non-Newt. Fluid Mech.*, 2014, **212**(0), 36–46.
8. Renner, B., Altenbach, H., and Naumenko, K. Rotation of an axisymmetric particle in a plane flow. *PAMM*, 2011, **11**(1), 333–334.
9. Altenbach, H., Naumenko, K., Pylypenko, S., and Renner, B. Influence of rotary inertia on the fiber dynamics in homogeneous creeping flows. *ZAMM – J. Appl. Math. Mech.*, 2007, **87**(2), 81–93.
10. Bentur, A. and Mindess, S. *Fibre Reinforced Cementitious Composites*. Spon Press, 1990.
11. Bentur, A. and Mindess, S. *Fibre Reinforced Cementitious Composites*. Taylor & Francis, London and New York, 2007.
12. Tejchman, J. and Kozicki, J. *Experimental and Theoretical Investigations of Steel-Fibrous Concrete*. 1st ed., Springer, 2010.
13. Herrmann, H., Eik, M., Berg, V., and Puttonen, J. Phenomenological and numerical modelling of short fibre reinforced cementitious composites. *Meccanica*, 2014, **49**(8), 1985–2000.
14. Eik, M., Puttonen, J., and Herrmann, H. An orthotropic material model for steel fibre reinforced concrete based on the orientation distribution of fibres. *Compos. Struct.*, 2015, **121**, 324–336.
15. Schnell, J., Schladitz, K., and Schuler, F. Richtungsanalyse von Fasern in Betonen auf Basis der Computer-Tomographie. *Beton- Stahlbetonbau*, 2010, **105**(2), 72–77.
16. Ponikiewski, T., Katzer, J., Bugdol, M., and Rudzki, M. Steel fibre spacing in self-compacting concrete precast walls by X-ray computed tomography. *Mater. Struct.*, 2015, **48**(12), 3863–3874.
17. Gödde, L., Strack, M., and Mark, P. Bauteile aus Stahlfaserbeton und stahlfaserverstärktem Stahlbeton. *Beton- Stahlbetonbau*, 2010, **105**(2), 78–91.
18. Michels, J., Maas, S., Zürbes, A., and Waldmann, D. Tragverhalten von Flachdecken aus Stahlfaserbeton im negativen Momentenbereich und Bemessungsmodell für das Gesamtsystem. *Beton- Stahlbetonbau*, 2010, **105**(8), 496–508.
19. Suuronen, J. P., Kallonen, A., Eik, M., Puttonen, J., Serimaa, R., and Herrmann, H. Analysis of short fibres orientation in Steel Fibre Reinforced Concrete (SFRC) using X-ray tomography. *J. Mater. Sci.*, 2013, **48**(3), 1358–1367.
20. Eik, M., Löhmus, K., Tigasson, M., Listak, M., Puttonen, J., and Herrmann, H. DC-conductivity testing combined with photometry for measuring fibre orientations in SFRC. *J. Mater. Sci.*, 2013, **48**(10), 3745–3759.
21. Vicente, M. A., González, D. C., and Mínguez, J. Determination of dominant fibre orientations in fibre-reinforced high-strength concrete elements based on computed tomography scans. *Nondestruct. Test. Eval.*, 2014, **29**(2), 164–182.
22. Eik, M. and Herrmann, H. Raytraced images for testing the reconstruction of fibre orientation distributions. *Proc. Estonian Acad. Sci.*, 2012, **61**, 128–136.
23. Chi, Y., Xu, L., and Sui, Yu. H. Constitutive modeling of steel-polypropylene hybrid fiber reinforced concrete

- using a non-associated plasticity and its numerical implementation. *Compos. Struct.*, 2014, **111**, 497–509.
24. Won, J. P., Hong, B. T., Lee, S. J., and Choi, S. J. Bonding properties of amorphous micro-steel fibre-reinforced cementitious composites. *Compos. Struct.*, 2013, **102**, 101–109.
 25. Krasnikovs, A., Zaharevskis, V., Kononova, O., Lasis, V., Galushchak, A., and Zaleskis, E. Fiber concrete properties control by fibers motion investigation in fresh concrete during casting. In *8th International DAAAM Baltic Conference "INDUSTRIAL ENGINEERING"* 19–21 April 2012, Tallinn, Estonia. 2012, 6 pages.
 26. Macanovskis, A. *Short Fiber Composite Internal Geometry Influence on the Material's Load Bearing Capacity and Strength*. PhD thesis, Institute of Mechanics, Faculty of Transport and Mechanical Engineering, Riga Technical University, 2014.
 27. Van Zijl, G. P. A. G. and Zeranka, S. The impact of rheology on the mechanical performance of steel fiber-reinforced concrete. In *HPFRCC 6* (Parra-Montesinos, G. J., Reinhardt, H. W., and Naaman, A. E., eds), *RILEM*, 2012, 59–66.
 28. Øfsdahl, E. *Fibre-Reinforced Self-Compacting Concrete: Prediction of Rheological Properties*. MSc thesis in Civil and Environmental Engineering, Department of Structural Engineering, Norwegian University of Science and Technology, 2012.
 29. Laskar, A. I. and Talukdar, S. Rheology of steel fiber reinforced concrete. *Asian J. Civil Engin. (Building Housing)*, 2008, **9**(2), 167–177.
 30. Martinie, L., Rossi, P., and Roussel, N. Rheology of fiber reinforced cementitious materials: classification and prediction. *Cement Concrete Res.*, 2010, **40**(2), 226–234.
 31. Boulekbache, B., Hamrat, M., Chemrouk, M., and Amziane, S. Flowability of fibre-reinforced concrete and its effect on the mechanical properties of the material. *Constr. Build. Mater.*, 2010, **24**(9), 1664–1671.
 32. Švec, O., Skoček, J., Olesen, J. F., and Stang, H. Fibre reinforced self-compacting concrete flow simulations in comparison with L-box experiments using carbo-pol. In *8th RILEM International Symposium on Fiber Reinforced Concrete: Challenges and Opportunities (BEFIB 2012)* (Barros, Y. A. O., ed.), *RILEM Publications SARL*, 2012, 897–905.
 33. Švec, O. *Flow Modelling of Steel Fibre Reinforced Self-Compacting Concrete – Simulating Fibre Orientation and Mechanical Properties*. PhD thesis. Department of Civil Engineering, DTU, 2013. Available from <http://www.byg.dtu.dk/english/~ /media/Institutter /Byg/publikationer/PhD/byg-r289.ashx> (accessed 17 October 2015).
 34. Hess, S. and Köhler, W. *Formeln zur Tensor-Rechnung*. Palm & Enke, Erlangen, 1980.
 35. Advani, S. G. and Tucker, III C. L. The use of tensors to describe and predict fiber orientation in short fiber composites. *J. Rheol.*, 1987, **31**(8), 751–784.
 36. Ehrentraut, H. and Muschik, W. On symmetric irreducible tensors in d-dimensions. *ARI – An Int. J. Phys. Eng. Sci.*, 1998, **51**(2), 149–159.
 37. Herrmann, H. and Eik, M. Some comments on the theory of short fibre reinforced materials. *Proc. Estonian Acad. Sci.*, 2011, **60**(3), 179–183.
 38. Heinen, K. *Mikrostrukturelle Orientierungszustände strömender Polymerlösungen und Fasersuspensionen*. PhD thesis. Universität Dortmund, 2007.
 39. Folgar, F. and Tucker, C. L. Orientation behavior of fibers in concentrated suspensions. *J. Reinf. Plast. Comp.*, 1984, **3**(2), 98–119.
 40. Chung, D. H. and Kwon, T. H. Invariant-based optimal fitting closure approximation for the numerical prediction of flow-induced fiber orientation. *J. Rheol.*, 2002, **46**(1), 169–194.
 41. Damián, S. M. *An Extended Mixture Model for the Simultaneous Treatment of Short and Long Scale Interfaces*. PhD thesis. Universidad Nacional del Litoral, Santa Fe, Argentina, 2013. Available from http://bibliotecavirtual.unl.edu.ar:8180/tesis/bitstream/1/489/3/Santiago_Marquez_Damian_PhD.pdf (accessed 17 October 2015).
 42. Švec, O. *4C-Flow*. 2014; <http://www.dtu.dk/4c-flow/examples/33808,2?example=SquarePlateNoRein> (accessed 17 October 2015).
 43. Eik, M. *Orientation of Short Steel Fibres in Concrete: Measuring and Modelling*. PhD thesis. Faculty of Civil Engineering, Institute of Cybernetics at Tallinn University of Technology, and Aalto University School of Engineering, 2014. Available from <http://digi.lib.ttu.ee/file.php?DLID=965> (accessed 17 October 2015).

Reoloogilise ääretingimuse mõju terasfibri orientatsioonile kiudbetoonelementide tootmisprotsessil

Heiko Herrmann ja Aarne Lees

On käsitletud reoloogilisi simulatsioone ja ääretingimuse mõju terasfibri suunajaotusele kiudbetooni valuprotsessil. Pinna karedusastmel võib teraskiudude orientatsioonile olla oluline mõju. Seega tuleb kiudbetooni valuvormide puhul arvesse võtta vormide materjali- ja pinnaomadusi. Samuti avaneb võimalus mõjutada teraskiudude orientatsiooni, valides sobivate pinnaomadustega valuvorme.